Available online at www.sciencedirect.com
ScienceDirect
Biochemical and Biophysical Research Communications 349 (2006) 416–425
BBRC
www.elsevier.com/locate/ybbrc

Endotoxin-induced nitric oxide production rescues airway growth and maturation in atrophic fetal rat lung explants ☆

C. Rae, J.I. Cherry, F.M. Land, S.C. Land *

Division of Maternal and Child Health Sciences, Ninewells Hospital and Medical School, University of Dundee, Dundee, DD1 9SY Scotland, UK

Received 11 August 2006
Available online 22 August 2006

Abstract

Inflammation induces premature maturation of the fetal lung but the signals causing this effect remain unclear. We determined if nitric oxide (NO) synthesis, evoked by *Escherichia coli* lipopolysaccharide (LPS, 2 μg ml^{-1}), participated in this process. Fetal rat lung airway surface complexity rose 2.5-fold over 96 h in response to LPS and was associated with increased iNOS protein expression and activity. iNOS inhibition by N6-(1-iminoethyl)-L-lysine-2HCl (L-NIL) abolished this and induced airway atrophy similar to untreated explants. Surfactant protein-C (SP-C) expression was also induced by LPS and abolished by L-NIL. As TGFβ suppresses iNOS activity, we determined if feedback regulation modulated NO-dependent maturation. LPS induced TGFβ1 release and SMAD4 nuclear translocation 96 h after treatment. Treatment of explants with a blocking antibody against TGFβ1 sustained NO production and airway morphogenesis whereas recombinant TGFβ1 antagonized these effects. Feedback regulation of NO synthesis by TGFβ may, thus, modulate airway branching and maturation of the fetal lung.

Keywords: Lipopolysaccharide; Nitric oxide; Transforming growth factor β; Lung development; Airway morphogenesis

Inflammation is known to improve lung maturation and function in premature newborns despite an attendant risk of premature delivery and postnatal respiratory disease [1,2]. Several studies have shown that inflammatory stimuli *in utero* increase alveolar type II (ATII) cell number, surfactant production and improve pulmonary function in premature neonates [3–7]. Dissection of these effects has revealed particular roles for interleukin (IL)1 and toll-like receptor 4 (TLR4) activation in stimulating alveologenesis [4,8,9]. In addition, manipulation of the cytokine expression pattern induced by LPS redirects airway growth by modulating meso-epithelial morphogenic signalling [10]. These findings suggest that pro-inflammatory signals can influence the process of fetal lung development, however, the identity of the factors responsible for this effect remains unclear.

Nitric oxide (NO) is an important mediator of inflammation which participates in lung development and morphogenesis. All three nitric oxide synthase isoforms (inducible (i), endothelial (e), and neuronal (n)) are ontogenically expressed in lung tissues [11] and prominently regulate several aspects of postnatal lung function including bronchomotor tone, regulation of ciliary beat frequency, bacteriostasis, and fluid homeostasis [12–15]. In the fetal lung, however, the functional significance of NO synthesis remains unknown. Correlative studies suggest that NO could participate in lung fluid clearance and airway expansion by, respectively, suppressing Cl^- transport and reducing peripheral resistance in the newborn [16]. Other studies demonstrate that exposure of fetal lung explants to exogenous NO derived from NO donor adducts (e,g., DETA-NO) can augment airway branching morphogenesis, possibly by modulating the expression of some meso-epithelial

☆ *Abbreviations:* ASC, airway surface complexity; DAF-FM, 4-amino-5-methylamino-2′,7′-difluorofluorescein; DETA-NO, 2,2′-[hydroxynitrosohydrazono]bis-ethanimine; DMEM, Dulbecco's modified Eagle's medium; FITC, fluorescein isothiocyanate; iNOS, inducible nitric oxide synthase; L-NIL, N6-(1-iminoethyl)-L-lysine dihydrochloride; LPS, lipopolysaccharide; SP-C, surfactant protein-C; TGFβ, transforming growth factor β.

* Corresponding author. Fax: +44 0 1382 425554.
E-mail address: s.c.land@dundee.ac.uk (S.C. Land).

0006-291X/$ - see front matter © 2006 Elsevier Inc. All rights reserved.
doi:10.1016/j.bbrc.2006.08.067

growth factors (e,g., BMP4) [17,18]. This morphogenic effect is also evident in the process of alveologenesis which is promoted by inhalation of NO in neonatal models of chronic lung disease [19,20]. As a whole, these studies support the hypothesis that NO can modulate the lung developmental/morphogenic process.

Here, we sought to determine if endogenous production of NO in the fetal lung could promote airway growth and maturation in fetal rat lung explants cultured under conditions which promote airway atrophy. We found that LPS halted the decline in airway growth and that this effect required endogenous NO synthesis by iNOS. We also showed that this signalling pathway was repressed by transforming growth factor β (TGFβ) expressed as a chronic effect of LPS. We conclude that the extent of airway maturation and growth that may be induced by LPS depends on a time- and concentration-dependent feedback inhibition of NO synthesis by TGFβ1.

Material and methods

Reagents. Antibodies raised against iNOS (M-19), TGFβRI (H-100), and TGFβRII (H-567), TGFβRIII (C-20), TGFβ1 (V), SMAD4 IgG (B-8), and SP-C (M20) were from Santa Cruz Biotechnology Inc (Santa Cruz, CA). Anti-rabbit β-actin was from Sigma–Aldrich (Gillingham, Dorset, UK). Horseradish peroxidase (HRP)- and fluorescein isothiocyanate (FITC)-conjugated secondary antibodies were from Diagnostics Scotland (Carluke, Lanarkshire, UK). Oligonucleosome detection ELISA was from Roche Diagnostics (East Sussex, UK) and TGFβ1 ELISA was from R&D Systems (Abingdon, UK). 4-Amino-5-methylamino-2′,7′-difluorofluorescein (DAF-FM) was from Molecular Probes (Cambridge, UK). L-[^{14}C(U)]Arginine (specific activity 313 mCi mmol^{-1}) was from Perkin-Elmer Life Sciences (Boston, MA). Phosphothioated iNOS and random sequence control antisense oligodeoxynucleotides were from Biognostik (Göttingen, Germany). Culture solutions and antibiotics were from GibcoBRL Life Technologies Inc (Paisley, UK). All other bench chemicals were purchased from Sigma–Aldrich (Dorset, UK).

Culture of lung explants and A549 cells. Lung explants from gestation (G) day 13 or 14 Sprague–Dawley rat fetuses were cultured as previously described [10] in a humidified atmosphere containing 5% CO_2 and 21% O_2. Digital images were captured at the start and end of each experiment using a Leica DC 300F digital camera mounted on a MZ FLIII binocular microscope under identical magnification settings (Leica Camera Ltd, Milton Keynes, UK). Human lung ATII-like adenocarcinoma A549 cells and human embryonic lung fibroblast HEL12469 cells were maintained in filter-capped Cellstar 75 cm^2 flasks (Greiner Bio-one, Frickhausen, Germany) in DMEM supplemented with 10% fetal calf serum and 100 U ml^{-1} penicillin/streptomycin. Cultures were routinely passaged within 90% confluence.

Reporter genes. A surfactant protein-C promoter-driven reporter gene was constructed by cloning a *Hin*dIII fragment containing 3.7 kb of the human surfactant protein-C promoter from pUC3.7hSP-C (kindly provided by J. Whitsett, Children's Hospital, Cincinatti) into the corresponding restriction site upstream of pd2EGFP (Clontech). The resulting vector (p3.7SP-C-d2EGFP) contained the SP-C promoter upstream of a gene encoding a destabilized variant of green fluorescent protein (d2EGFP, $t1/2 = 2$ h). Transfection of A549 cells and explants was performed using Lipofectamine 2000 (Invitrogen, Paisley, UK). The development of fluorescence over time was determined in A549 cells by direct measurement using a Fluostar Optima fluorescent plate reader (BMG Labtek, Aylesbury, UK). In transfected explants, the distribution and intensity of fluorescence in explants was determined using a Leica MZ FLIII fluorescent binocular microscope equipped with GFP resolving filters. Identical magnification, contrast, and gain settings were maintained throughout. The procedure for iNOS knockdown using phosphorothioated antisense oligodeoxynucleotides (ODN) was as previously described [21]

TGFβ bioactivity was determined using the 3TP-Lux luciferase vector (kindly provided by J. Massague, Howard Hughes Medical Institute, Memorial Sloan-Kettering Cancer Center, New York) transfected into HEL12469 cells. Results were referenced against the *Renilla* luciferase vector (pRL, Promega).

Morphometry and immunohistochemistry. Airway surface complexity [ASC; perimeter (mm)/$\sqrt{}$area (mm^2)] was determined from digital images using Scion Image 4.0.2 software (Scion Corporation, Frederick, MD) [10]. Change in the surface area fraction of the major structural features of the lungs (epithelium, mesenchyme, and airway space) was determined from haematoxylin and eosin, stained histochemical sections as before [10]. Immunohistochemistry was performed on filter-attached explants fixed for 30 min in a solution of PBS containing 10% formalin (pH 7.2). After sectioning, antigen retrieval, and blocking, sections were probed overnight with the appropriate primary antibody at 1:50 dilution. Negative controls were conducted using BSA alone. Immunodetection was performed on TBS-washed immuno-reacted sections using either anti-IgG-FITC or anti-IgG-DAB-conjugated secondary antibodies at 1:200 dilution. Images were obtained using a Zeiss Axioscope confocal microscope (Zeiss, Herts, UK). The contrast properties were optimized for each section and then referenced against the retrospective negative control image using identical camera and microscope settings.

Bromodeoxyuridine (BrdU) labelling. The distribution of mitotic cell activity was determined by following the incorporation of BrdU using a fluorescent *In Situ* Cell Proliferation Kit (Roche Diagnostics GmbH, Mannheim, Germany). Briefly, 10 μM BrdU was added to the medium in contact with explants and was incorporated for 24 h under various treatment regimen. At the end of this period, explants were processed as described for *Immunohistochemistry* and BrdU incorporation into nuclei was resolved using an anti-BrdU-FLUOS monoclonal antibody. Fluorescent and bright field images from each section were obtained using a Zeiss LSM-510 confocal microscope.

Determination of apoptosis. Apoptosis was determined in lysed explants using an oligonucleosome detection ELISA as before [10].

Nitrite production, iNOS activity, and DAF-FM fluorescence. Nitrite accumulation and iNOS activity assays were determined using the Griess assay and by following the rate of [^{14}C]arginine conversion to citrulline were as described before [21]. NO production in intact explants was examined using the NO-sensitive fluorescent dye, DAF-FM. 10 μM DAF-FM was added to the medium beneath the explant and the culture dish was returned to the darkened culture chamber for 1 h. Explants were then washed free of unincorporated dye and then treated as indicated. Images were obtained using the Leica MZ FLIII fluorescent binocular microscope with dye excitation at 488 nm and emitted light detected at 535 nm. The use of this dye to detect NO production in living tissue has been validated by us previously [21].

Western blotting. Cytoplasmic and nuclear fractions were extracted from explants using a Nuclear Extract Kit (Active Motif, Rixensart, Belgium) according to the manufacturer's instructions. Total protein content of these fractions was determined using the Bio-Rad protein assay (Bio-Rad) and equal quantities of protein were loaded in each lane. Even transfer of proteins onto nitrocellulose was confirmed by staining with Ponceau S. Immunodetection of blotted proteins was as described by us previously [10,21].

TGFβ1 ELISA. Release of TGFβ1 from lysed explant samples was determined using an R&D Systems (Abingdon, UK) ELISA for mouse/rat/porcine TGFβ1. Briefly, explants were lysed by sonicating in lysis buffer containing protease inhibitor cocktail (Roche Diagnostics, East Sussex, UK) and, after activation, duplicate samples were added to a microplate pre-coated with TGFβ1 monoclonal antibody. The optical density was determined at 450 nm, with wavelength correction at 550 nm using a Dynatech Laboratories (Guernsey, UK) MRX microplate reader. TGFβ1 concentrations were calculated from a standard curve and equalized for protein content.

Data handling and statistics. Data are presented as means ± standard error (SEM) with the number of independent repetitions provided in the legend to each figure. Statistical analysis was assessed relative to control groups using one-way analysis of variance with the level of significance determined using the post hoc Tukey's honestly significant difference.

Results

Effect of LPS upon airway branching

G14 Fetal rat lung explants were exposed to a range of LPS concentrations (0.5–50 μg ml^{-1}) for 96 h. Untreated explants atrophied severely over this time and developed large peripheral epithelium-lined fluid-filled structures (Fig. 1A). ASC rose by ~1.5-fold over the 96 h period reflecting an overall increase in the gross mass of the explant but there was no observable increase in airway branching (Fig. 1B). By comparison, low concentrations of LPS (0.5 and 2 μg ml^{-1}) evoked a ~2-fold change in ASC with dichotomous airway branching penetrating to the explant periphery (Figs. 1A and B). Higher concentrations of LPS (10 and 50 μg ml^{-1}) abolished airway branching and resulted in an amorphous, solid tissue mass (Figs. 1A and B).

The proportion of surface area occupied by airway space, epithelium, and mesenchyme was determined from fixed sections of the same experimental set of explants.

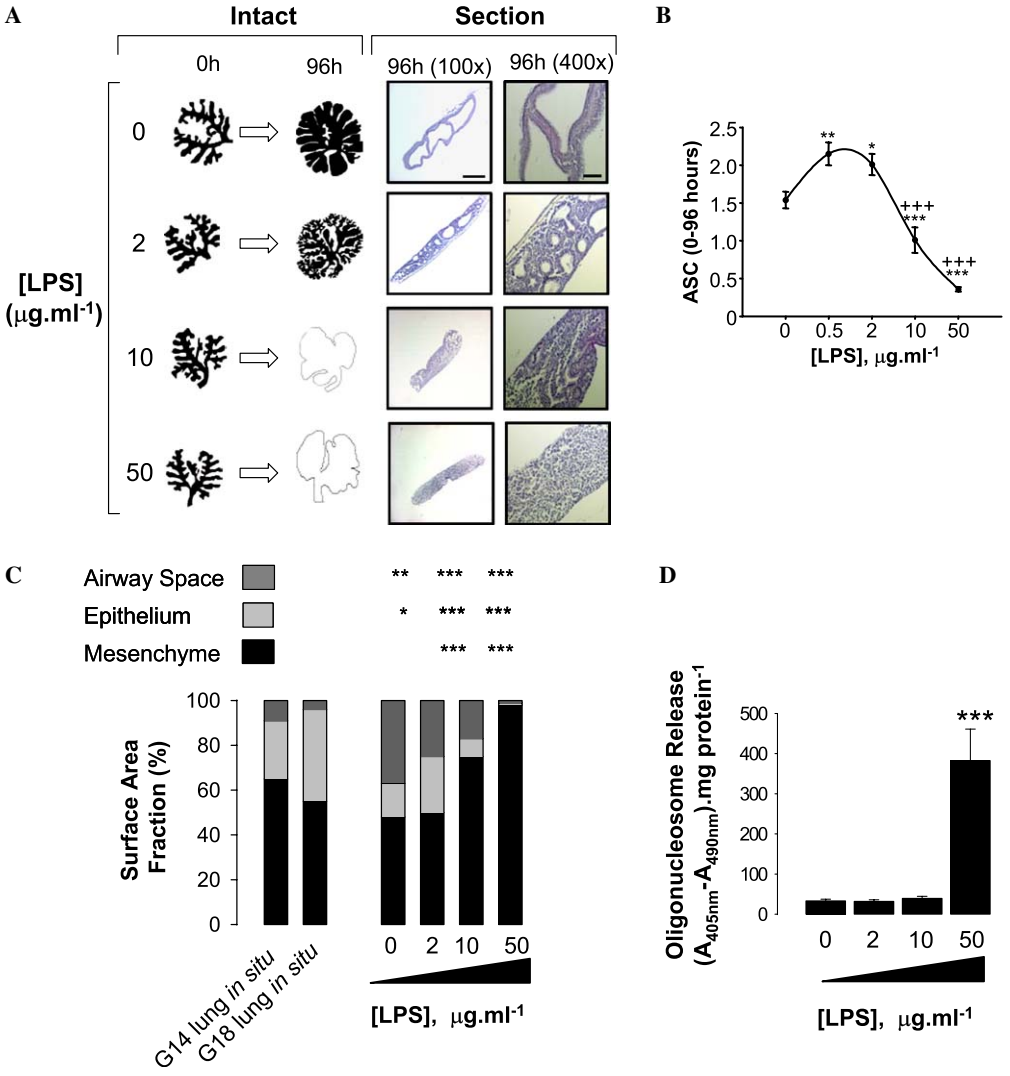

Fig. 1. Effect of LPS on fetal rat lung explant morphology. (A) Representative images showing the extent of airway bifurcation in intact G14 explants cultured for 96 h at the indicated LPS concentrations. Images are space-filled tracings of the airway perimeter; grey silhouettes represent outline of solid explant mass where no airway structures were evident. H&E-stained sections reveal the distribution of airway epithelium, mesenchyme, and airway space in explants exposed to each treatment. Bar = 100 μm (section at 100× magnification) and 25 μm (section at 400× magnification). (B) Effect of LPS (0.5–50 μg ml^{-1}) on airway surface complexity (ASC 0–96 h). ASC was calculated as airway perimeter (mm)/$\sqrt{}$airway area (mm^2) ($N = 9$, $^{*}p < 0.05$, $^{**}p < 0.01$, and $^{***}p < 0.001$ *vs* control, $^{+++}p < 0.001$ *vs* 2 μg ml^{-1} LPS). (C) Effect of LPS upon the percentage of explant section surface area occupied by mesenchyme, epithelium or airway space. The same surface area proportions from sections of native G14 and G18 lungs are shown for comparison. Mean values only are shown for clarity ($N = 9$. $^{*}P < 0.05$, $^{**}P < 0.01$, and $^{***}P < 0.001$ *vs* respective untreated group). (D) Effect of LPS upon explant apoptosis. Histogram shows oligonucleosome release after 96 h exposure of explants to LPS at the concentrations indicated ($N = 7$. $^{***}p < 0.001$ *vs* untreated controls).

For comparison, these data are shown with the same surface area proportions calculated from sections of native lung tissue from G14 and G18 fetuses (Fig. 1C). Epithelial surface area fraction increased significantly ($P < 0.01$) following exposure to 2 μg ml^{-1} LPS relative to untreated explants, whereas 10 μg ml^{-1} LPS evoked significant mesenchyme thickening and epithelial atrophy. LPS (50 μg ml^{-1}) abolished all recognizable airway structures and induced mesenchyme proliferation coupled with widespread apoptosis (Fig. 1D).

LPS induction of NO synthesis

LPS (2 μg ml^{-1}) (optimal concentration for airway growth, Fig. 1A) induced iNOS protein expression, activity, and NO release within 24 h (Figs. 2A and B). NO production in intact explants was visualized using the NO fluorescent dye, DAF-FM (Fig. 2C). Fluorescence was present only in the proximal airway region in control explants, however, LPS raised the level of fluorescence in the distal airways and around the growth region of the terminal airway bud (arrows). The iNOS specific inhibitor, L-NIL, abolished both DAF-FM fluorescence and nitrite production induced by LPS.

LPS-evoked NO production induces airway branching and epithelial cell maturation

To determine if NO synthesis was necessary for the rise in ASC induced by endotoxin-induced inflammation, the effect of L-NIL was examined on LPS-induced morphological events. L-NIL abolished airway branching induced by 2 μg ml^{-1} LPS and lowered both ASC and the epithelial surface area fraction (Fig. 3A). Proliferation of epithelial and mesenchyme tissue, measured by BrdU uptake, was widespread in LPS-treated explants, but abolished by L-NIL (Fig. 3B).

The effect of these treatments on epithelial function was determined by following the expression and distribution of surfactant protein C (SP-C). In ATII-like A549 cells, 0.5 μg ml^{-1} LPS was sufficient to evoke a maximal rate of pSP-C3.7d2EGFP reporter gene expression which was

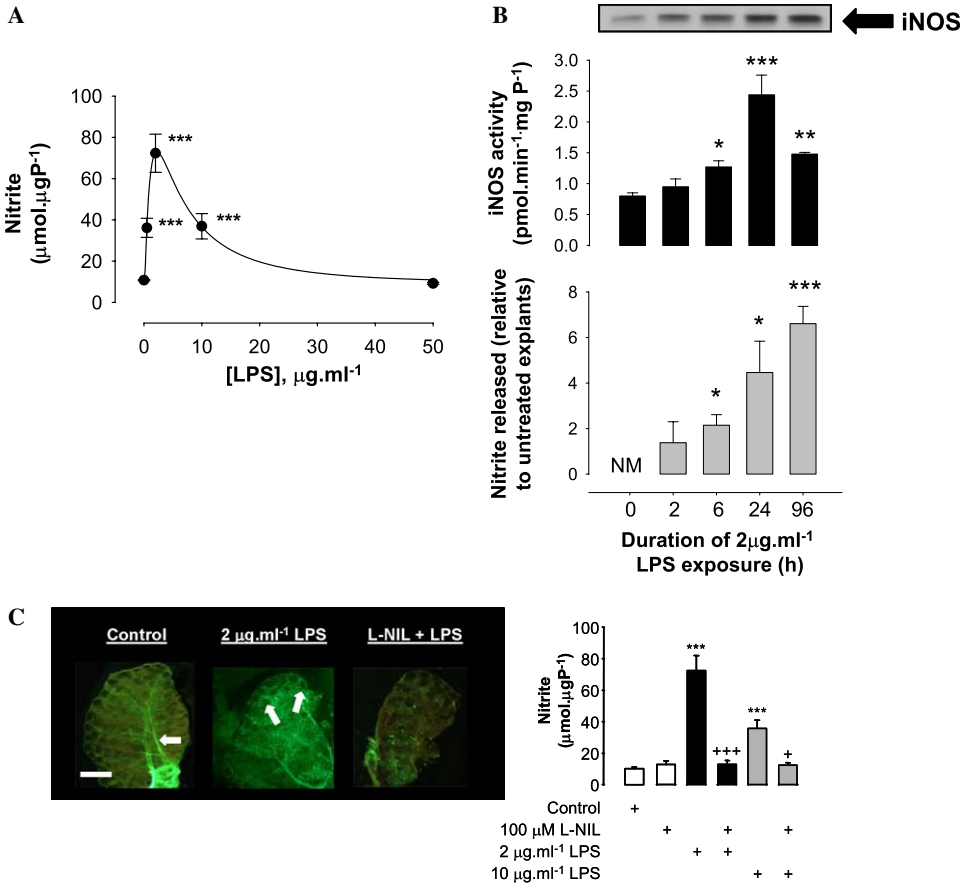

Fig. 2. Effect of LPS on iNOS activity and NO production release from fetal rat lung explants. (A) Effect of LPS upon nitrite production [by Greiss assay ($n = 4$, $^{***}P < 0.001$ vs 0LPS)]. (B) Timecourse of LPS (2 μg ml^{-1}) induced iNOS protein expression (upper blot), iNOS activity (upper histogram), and nitrite release (lower histogram) ($N = 4$, $^{*}p < 0.05$, $^{**}p < 0.01$, $^{***}p < 0.001$ *vs* untreated controls). (C) Visualization of NO production (as spontaneous DAF-FM fluorescence) in living explants exposed to LPS (2 μg ml^{-1}) and the iNOS inhibitor, L-NIL (100 μM). Images representative of three independent experiments. White arrow indicates proximal and distal regions of fluorescence. Bar = 250μm. Histogram shows the inhibition of NO production by L-NIL ($N = 8$. $^{***}p < 0.001$ *vs* untreated control, $^{+++}p < 0.001$ *vs* 2 μg ml^{-1} LPS, and $^{+}p < 0.05$ *vs* 10 μg ml^{-1} LPS).

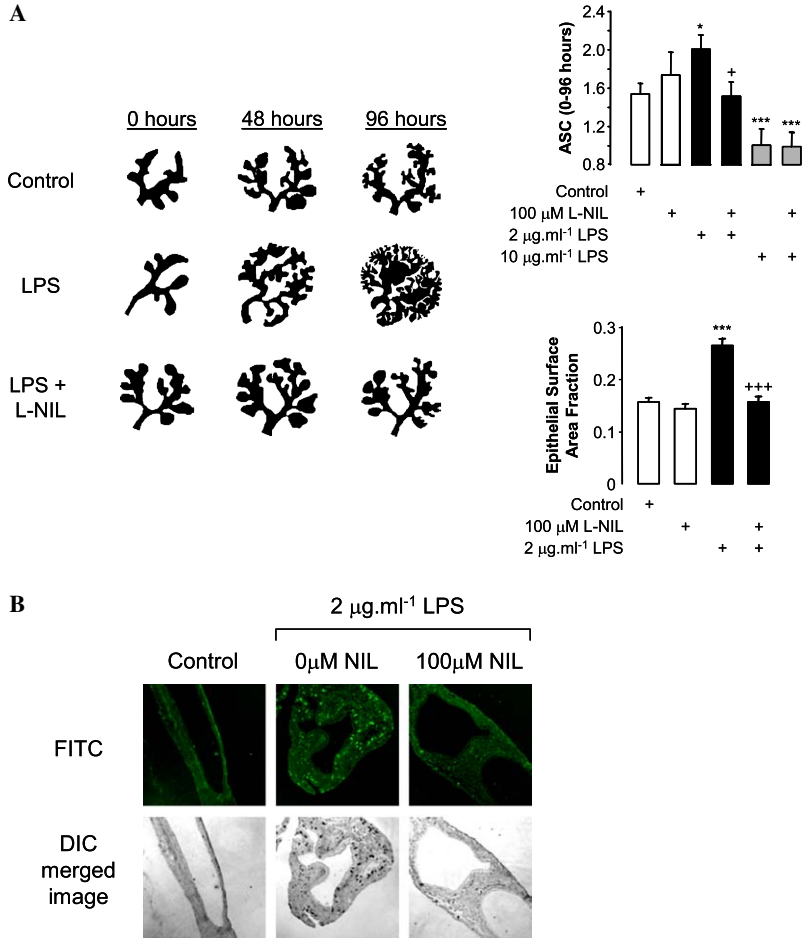

Fig. 3. Effect of L-NIL on LPS-induced explant morphology. (A) Representative images showing the extent of airway branching over time on exposure to 0 or 2 μg ml^{-1} LPS ± 100 μM L-NIL of G13 explants. Images are space-filled tracings of the airway perimeter. Histograms show the quantitated effects of this treatment upon ASC (0–96 h) and epithelial surface area fraction at 96 h ($N = 6$, $^{*}p < 0.05$ and $^{***}p < 0.001$ *vs* untreated control, $^{+}p < 0.05$ and $^{+++}$<0.001 *vs* 2 μg ml^{-1} LPS). (B) Representative images ($N = 4$) showing the distribution of mitotic cell division in LPS and L-NIL treated explants. Explants were labelled with FITC-conjugated bromodeoxyuridine (BrdU) and then sectioned for microscopy. Upper panels, FITC fluorescence; lower panels, merged bright field image. BrdU incorporation in these images appears as black staining.

sustained at higher LPS concentrations (Fig. 4A). iNOS was the chief source of NO production as antisense knockdown of iNOS or L-NIL treatment abolished reporter gene expression (Fig. 4B). In fetal rat lung explants, 2 μg ml^{-1} LPS significantly raised SPC-promoted GFP expression within 24 h of treatment; this effect was abolished by L-NIL. Epithelial SP-C protein expression in explants was similarly induced by LPS and inhibited by L-NIL (Figs. 4C–E).

LPS-evoked TGFβ pathway activation and repression of NO production

TGFβ suppresses iNOS function and is crucial for normal lung morphogenesis. The expression and distribution of TGFβ receptors (TβR) I-III in explants was not altered by LPS treatment (data not shown). However, 2 μg ml^{-1} LPS induced a time-dependent increase in SMAD4 nuclear abundance and TGFβ1 expression (Fig. 5A) which reached statistical significance at 96h ($P < 0.05$, $n = 4$). Note that 2 μg ml^{-1} LPS was sufficient to induce SMAD4 nuclear translocation to its maximal extent (c.f. 100 ng ml^{-1} recombinant TGFβ1 (Fig. 5B)).

LPS-dependent TGFβ1 signalling was assessed using the p3TP-Lux reporter gene transfected into human embryonic lung fibroblasts and compared to SMAD4 nuclear translocation in fetal rat lung explants treated in parallel (Fig. 5C). LPS induced a 2-fold increase in 3TP-Lux reporter gene activity which was unaffected by L-NIL or the NO-donor adduct, DETA-NO. LPS induced SMAD4 nuclear translocation in explants was similarly insensitive to iNOS inhibition and exogenous NO.

TGFβ1 antagonizes NO-mediated morphogenesis in explants

To determine if the morphogenic effect of endogenous NO was altered by TGFβ1, we used an antibody derived against this growth factor to block its receptor interaction.

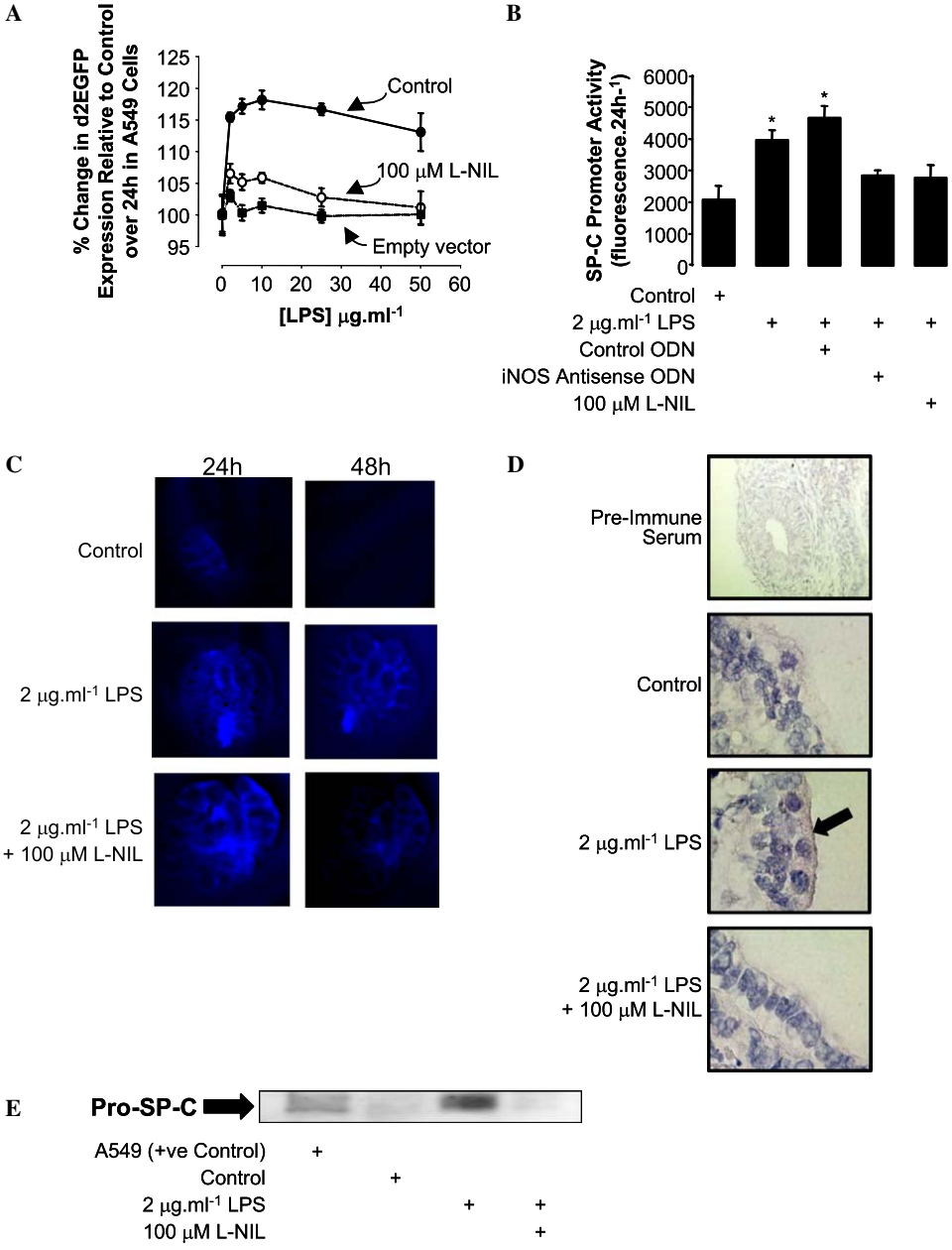

Fig. 4. Effect of LPS and L-NIL upon epithelial surfactant protein-C promoter activity and protein expression. (A) pSP-C3.7d2EGFP reporter gene activity in A549 cells treated with LPS (0.5–50 μg ml^{-1}) for 24 h in the absence or presence of L-NIL (100 μM), ($N = 6$). (B) pSP-C3.7d2EGFP reporter gene activity in A549 cells treated as for (A) with either random sequence control oligodeoxynucleotides (ODN) or iNOS antisense ODN (1 μM) 2 μg ml^{-1} LPS ± antisense oligonucleotides (control or iNOS) or L-NIL (100 μM), ($N = 6$, $^{*}P < 0.05$ *vs* control). (C) pSP-C3.7d2EGFP reporter gene in living explants treated as in (A). Each representative image ($N = 4$) shows the same explant photographed at 24 and 48 h of culture. (D) SP-C protein expression (black arrow) in explant airway epithelium. Explants were treated as in (A) for 48 h then processed for immunohistochemistry ($N = 3$). (E) Pro-SP-C protein expression in protein lysates from fetal rat lung explants treated as in (A). A549 protein lysate was used as a positive control ($N = 3$).

Fig. 6A shows anti-IgG TGFβ1 abolished the LPS-induced rise in SMAD4 nuclear translocation in explants (blot above histogram) and also 3TP-lux activity in human lung fibroblasts; non-immune IgG had no effect. Treatment of LPS-exposed explants with recombinant TGFβ1 protein abolished iNOS protein expression, activity, and nitrite release, and inhibited the LPS-induced rise in airway surface complexity (Fig. 6B). Blockade of TGFβ1 signalling using anti-TGFβ1 IgG, however, did not augment the intensity of airway branching beyond the level observed with non-immune IgG.

Discussion

We have demonstrated that LPS sustains airway morphogenesis and epithelial determination (inferred from the expression of SPC) in fetal rat lung explants cultured under conditions which cause near total atrophy of lung

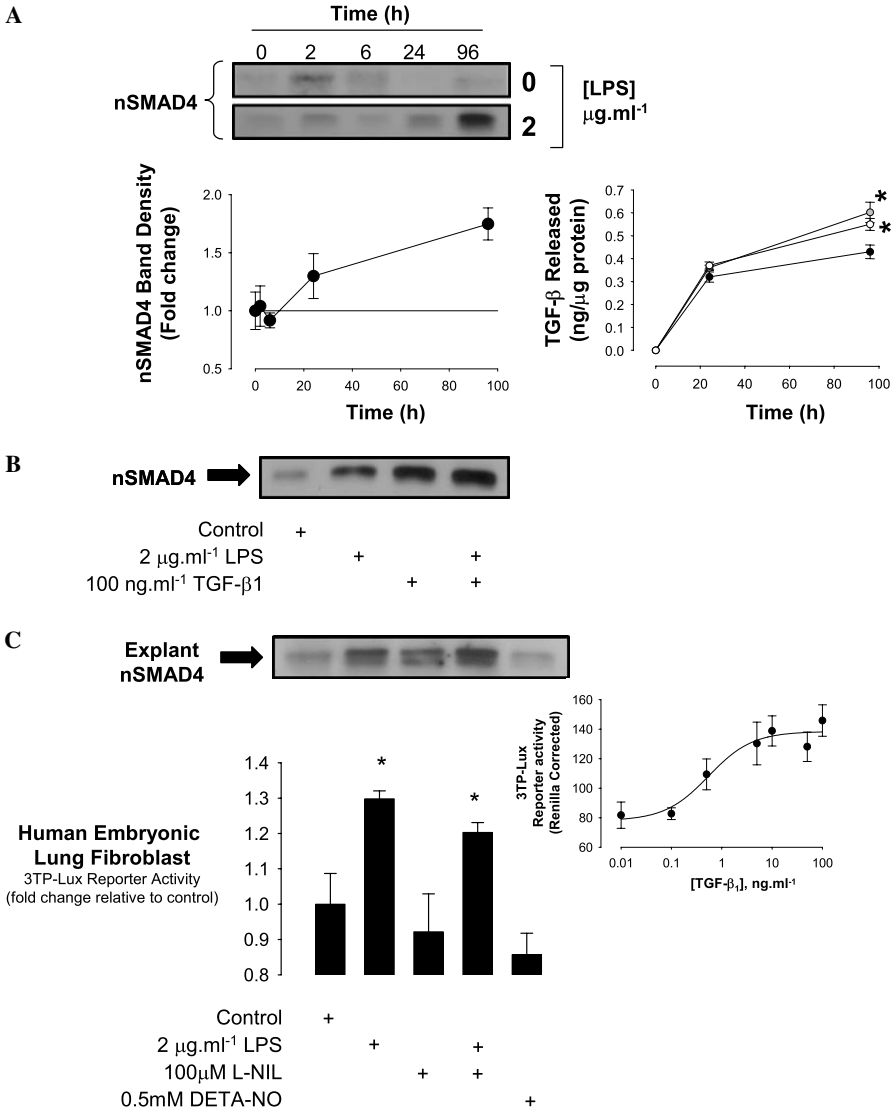

Fig. 5. Effect of LPS upon TGFβ receptor signalling in fetal rat lung explants. (A) Nuclear SMAD4 (nSMAD4) increases from 24 to 96 h following addition of 2 μg ml^{-1} LPS ($N = 3$). Graph on the right of the panel shows the parallel change in TGFβ1 release into the culture media over 96 h in response to 0 (filled circles), 2 (grey circles), and 10 (open circles) μg ml^{-1} LPS ($N = 5$, $^{*}P < 0.05$ vs 24 h point). (B) LPS (2 μg ml^{-1}) maximally induces nSMAD4 (representative of $N = 3$ independent experiments). (C) Effect of LPS, L-NIL, and the NO donor adduct, DETA-NO, upon fetal rat lung explant nSMAD4 abundance (upper blot) and human embryonic lung fibroblast 3TP-Lux reporter gene expression (histogram) ($N = 4$, $^{*}P < 0.05$ *vs* control). Inset, titration of reporter gene activity in fibroblasts exposed for 6 h to 0.01 → 100 ng ml^{-1} recombinant TGFβ1 ($N = 4$).

structure. This effect involved iNOS-dependent NO production from non-immune cells of the lung and was antagonized by the later expression of TGFβ1. Although the explant culture model is inevitably removed from the lung *in vivo*, these data demonstrate that an inflammatory stimulus directed at the epithelial and mesenchymal tissues of the lung potently modulates the growth process of the lung to favour airway elongation and division. Previous studies have demonstrated a similar effect using long half-life NO donor compounds (e,g., DETA-NO: (*Z*)-1-[2-(2-aminoethyl)-*N*-(2-ammonioethyl)amino]-diazen-1-ium-1,2-diolate NO) and broad-spectrum NOS inhibitors have been shown to inhibit spontaneous airway growth in explants [17,18]. Here, we demonstrate that endogenous sources of NO synthesis are sufficient to promote airway branching and epithelial cell functional determination. Both of these effects were blocked by the specific iNOS inhibitor, L-NIL, and in the case of SP-C, were further specified to iNOS using antisense oligonucleotides. INOS is present in the proximal lung epithelium throughout gestation but only accounts for a significant proportion of the total NOS activity during the near-to-term canalicular and saccular stages of lung development [11]. This does not exclude the possibility that iNOS-generated NO may participate in localized trophic developmental signalling. Moreover, our results illustrate the potential for iNOS activation from the early pseudoglandular stage of lung development.

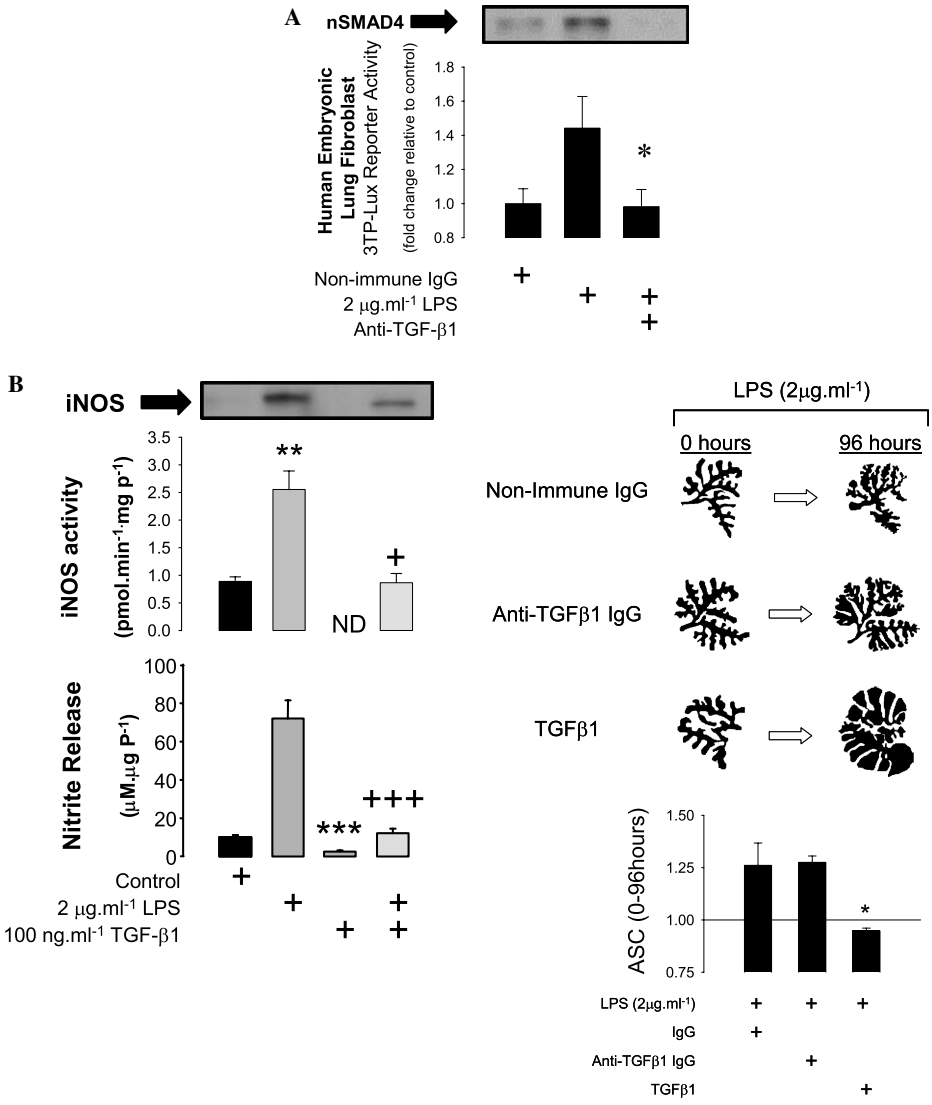

Fig. 6. TGFβ_1 antagonizes LPS-induced NO synthesis and airway morphogenesis. (A) Anti-IgG TGFβ_1 inhibits LPS-induced SMAD4 nuclear translocation in explants (upper blot) and 3TP lux reporter gene activity in human embryonic lung fibroblasts ($N = 4$, $^{*}P < 0.05$ relative to control). (B) LPS-induced iNOS protein expression, activity, nitrite release, and airway branching morphogenesis are inhibited by recombinant TGFβ1 (100 ng ml^{-1}). However, blockade of SMAD4 nuclear translocation using Anti-TGFβ1 IgG (1 μg ml^{-1}) does not augment LPS-induced airway branching beyond the level observed with non-immune IgG (1 μg ml^{-1}). Space-filled images show airway dimensions for each treatment with the corresponding change in airway surface complexity (ASC) for each of the treatments given in the histogram below, for iNOS activity and nitrite release histograms ($N = 11$; $^{**}P < 0.01$ relative to control, $^{+}P < 0.05$ relative to LPS treatment, $^{***}P < 0.001$ relative to LPS treatment, and $^{+++}P < 0.01$ relative to LPS treatment. ND, not detected) and $n = 3$ for ASC measurements ($^{*}P < 0.05$ relative to explants treated with non-immune IgG).

As well as conserving branching morphogenesis, our results show that the surface area fraction of differentiated epithelium was elevated by low concentrations of LPS and, after 96 h of culture, approximated the value observed at day 18 of gestation in native lung tissue; this is, again, indicative of a maturational effect. The production of pulmonary surfactant by alveolar epithelial cells is essential to maintain alveolar stability and normal lung function and its deficiency as a result of premature birth is directly linked to the development of neonatal respiratory distress syndrome [22]. Surfactant-associated proteins (SP-A, SP-B, SP-C, and SP-D) play a role in host defence and inflammation as well as influencing the surface tension-reducing properties [23]. SP-C is a commonly used marker of type II alveolar epithelial differentiation [24], and we demonstrated that both SP-C promoter activity and protein expression were induced by endotoxin. Endotoxin-induced increases in epithelial surface area, SP-C promoter activity, and SP-C protein expression were all abrogated by iNOS inhibition.

How NO might promote coordinated lung morphogenesis is unknown but likely targets include regulators of cell growth, apoptosis, trophic signals, and other inflammatory cytokines [25]. Lung morphogenesis requires reciprocal signalling interactions between the epithelium and the surrounding mesenchyme. These mesenchymal–epithelial

interactions are associated with changes in mesenchymal and epithelial cell proliferation and lung growth as well as associated regional changes in apoptosis. Recent studies have identified bone morphogenetic protein-4 (BMP-4) as one important morphogenic gene whose expression is induced by exogenous NO [17]. BMP-4 plays a critical role in proximal-distal cell differentiation and regulates epithelial cell proliferation along the axis of airway growth. Notably, its expression is confined to the distal growing regions of the airway, areas we have found which abundantly express iNOS protein, and is dynamically regulated with several other morphogenic genes (fibroblast growth factors 9 and 10, noggin, and sonic hedgehog) as a key element of the stereotypical airway branching process [26–29].

LPS concentrations greater than 10 $\mu g\,ml^{-1}$ abolished the NO-dependent morphogenic effect. Under oxidizing conditions, NO reacts with the superoxide radical to form peroxynitrite ($^{-}$OONO) which can activate a variety of pro-inflammatory signalling pathways [30], inhibit the lung development process [18], and cause acute lung injury [31,32]. However, we found that iNOS activity was suppressed after 96 h of exposure to 2 $\mu g\,ml^{-1}$ LPS and that nitrite production at 10 $\mu g\,ml^{-1}$ was approximately half of that produced at 2 $\mu g\,ml^{-1}$ LPS. We, therefore, hypothesized that a negative feedback mechanism was in place which functioned to protect against the detrimental effects of $^{-}$OONO in the developing lung.

TGFβ1 has been shown to act as a potent suppressor of endotoxin-induced NO production [33,34] through a mechanism which involves *Elk*-3 repression of iNOS mRNA synthesis [35]. The signal transduction pathway activated by TGFβ can involve several SMAD proteins whose interaction with the common effector, SMAD4, results in nuclear translocation and the modulation of target gene expression [36]. Fine tuning of this signal transduction pathway can occur by interaction with inhibitory SMAD6 or other growth factor pathways such as IGF2 and FGF8 [37]. We, therefore, examined SMAD4 nuclear translocation in explants as an indicator of TGFβ1 signalling and compared this effect with 3TP-Lux reporter gene expression in cultured fibroblasts. We found that TGFβ1 protein expression, nSMAD4 abundance, and reporter gene expression were induced by 2 $\mu g\,ml^{-1}$ LPS but that, in explants, this was temporally separated from NO induction. Thus, nitrite production and iNOS expression/activity were significantly elevated within 6 h of LPS treatment whereas TGFβ1 expression and nSMAD4 abundance were not induced until 96 h.

TGFβ regulates many processes including cellular proliferation and differentiation, inflammation, and wound repair [38]. In the fetal lung, TGFβ overexpression inhibits vascular development, arrests surfactant protein expression, and induces epithelial–mesenchymal transition [39–42]. In our experiments, recombinant TGFβ1 abolished the branching effect induced by low concentrations of LPS and also inhibited iNOS expression, activity, and nitrite release at the 96h time point. Inhibition of endogenous TGFβ1 production and signalling to SMAD4 using anti-IgG TGFβ1 antibody did not further augment the LPS-induced airway bifurcation, suggesting that the morphogenic effect was maximal under these conditions. Although it has been suggested that NO production may augment TGFβ activity [43], we found that endotoxin-induced SMAD4 nuclear translocation was unaffected by iNOS inhibition and DETA-NO, suggesting that an alternative acute inflammatory response phase signal is operative in the regulation of TGFβ expression (TNFα, for example [44]).

In conclusion, we have shown that endotoxin-evoked release of nitric oxide is involved in branching morphogenesis and lung maturation *ex vivo*. Activation of the TGFβ pathway by endotoxin, on the other hand, occurs independently of nitric oxide release and serves to maintain NO within a permissive range for fetal lung development. Although it is apparent that a number of growth factors are involved in fetal lung development, our data suggest that feedback regulation between NO- and TGFβ pathways plays a role in mesenchymal–epithelial interactions in the developing lung.

Acknowledgments

This work was supported by the Medical Research Council, Tenovus (Scotland) and the Anonymous Trust.

References

[1] K. Hannaford, D.A. Todd, H. Jeffery, E. John, K. Blyth, G.L. Gilbert, Role of Ureaplasma urealyticum in lung disease of prematurity, Arch. Dis. Child Fetal Neonatal Ed. 82 (1999) F162–F167.
[2] K.L. Watterburg, L.M. Demers, S.M. Scott, S. Murphy, Chorioamnionitis and early lung inflammation in infants in whom bronchopulmonary dysplasia develops, Pediatrics 97 (1996) 210–215.
[3] J.J. Pillow, A.H. Jobe, R.A. Collins, Z. Hantos, M. Ikegami, T.J. Moss, J.P. Newnham, K.E. Willet, P.D. Sly, Variability in preterm lamb lung mechanics after intra-amniotic endotoxin is associated with changes in surfactant pool size and morphometry, Am. J. Physiol. Lung Cell. Mol. Physiol. 287 (5) (2004) L992–L998.
[4] K. Bry, U. Lappalainen, M. Hallman, Intraamniotic interleukin-1 accelerates surfactant protein synthesis in fetal rabbits and improves lung stability after premature birth, J. Clin. Invest. 99 (1997) 2992–2999.
[5] B.W. Kramer, S. Kramer, M. Ikegami, A.H. Jobe, Injury, inflammation, and remodeling in fetal sheep lung after intra-amniotic endotoxin, Am. J. Physiol. Lung Cell. Mol. Physiol. 283 (2002) L452–L459.
[6] O. Vayrynen, V. Glumoff, M. Hallman, Regulation of surfactant proteins by LPS and proinflammatory cytokines in fetal and newborn lung, Am. J. Physiol. Lung Cell. Mol. Physiol. 282 (4) (2002) L803–L810.
[7] K.E. Willet, B.W. Kramer, S.G. Kallapur, M. Ikegami, J.P. Newnham, T.J. Moss, P.D. Sly, A.H. Jobe, Intra-amniotic injection of IL-1 induces inflammation and maturation in fetal sheep lung, Am. J. Physiol. Lung Cell. Mol. Physiol. 282 (2002) L411–L420.
[8] V. Glumoff, O. Vayrynen, T. Kangas, M. Hallman, Degree of lung maturity determines the direction of the interleukin-1-induced effect on the expression of surfactant proteins, Am. J. Respir. Cell. Mol. Biol. 22 (2000) 280–288.

[9] L.S. Prince, O.V. Okoh, T.O. Moninger, S. Matalon, Lipopolysaccharide increases alveolar type II cell number in fetal mouse lungs through Toll-like receptor 4 and NFκB, Am. J. Physiol. Lung Cell. Mol. Physiol. 287 (5) (2004) L999–L1006.
[10] S.C. Land, F. Darakhshan, Thymulin evokes IL-6-C/EBPβ regenerative repair and TNF-α silencing during endotoxin exposure in fetal lung explants, Am. J. Physiol. Lung Cell. Mol. Physiol. 286 (2004) L473–L487.
[11] P.W. Shaul, S. Afshar, L.L. Gibson, T.S. Sherman, J.D. Kerecman, P.H. Grubb, B.A. Yoder, D.C. McCurnin, Developmental changes in nitric oxide synthase isoform expression and nitric oxide production in fetal baboon lung, Am. J. Physiol. Lung Cell. Mol. Physiol. 283 (6) (2002) L1192–L1199.
[12] F.L. Ricciardolo, P.J. Sterk, B. Gaston, G. Folkerts, Nitric oxide in health and disease of the respiratory system, Physiol. Rev. 84 (3) (2004) 731–765.
[13] F.E. Aldwell, D.N. Wedlock, B.M. Buddle, Sequential activation of alveolar macrophages by IFN-γ and LPS is required for enhanced growth inhibition of virulent *Mycobacterium bovis* but not M. bovis BCG, Immunol. Cell Biol. 75 (2) (1997) 161–166.
[14] B. Jain, I. Rubinstein, R.A. Robbins, J.H. Sisson, TNF-α and IL-1β upregulate nitric oxide-dependent ciliary motility in bovine airway epithelium, Am. J. Physiol. 268 (6 Pt 1) (1995) L911–L917.
[15] M.N. Helms, L. Yu, B. Malik, D.J. Kleinhenz, C.M. Hart, D.C. Eaton, Role of SGK1 in nitric oxide inhibition of ENaC in Na^+-transporting epithelia, Am. J. Physiol. Cell Physiol. 289 (3) (2005) C717–C726.
[16] C.F. Potter, I.A. Dreshaj, M.A. Haxhiu, E.K. Stork, R.L. Chatburn, R.J. Martin, Effect of exogenous and endogenous nitric oxide on the airway and tissue components of lung resistance in the newborn piglet, Pediatr. Res. 41 (6) (1997) 886–891.
[17] M. Shinkai, T. Shinkai, M.A. Pirker, S. Montedonico, P. Puri, Effect of nitric oxide on fibroblast growth factor-10 and bone morphogenetic protein 4 expressions in the branching morphogenesis of fetal rat lung explants, J. Pediatr. Surg. 40 (6) (2005) 1030–1033.
[18] S.L. Young, K. Evans, J.P. Eu, Nitric oxide modulates branching morphogenesis in fetal rat lung explants, Am. J. Physiol. Lung Cell. Mol. Physiol. 282 (2002) L379–L385.
[19] D.C. McCurnin, R.A. Pierce, L.Y. Chang, L.L. Gibson, S. Osborne-Lawrence, B.A. Yoder, J.D. Kerecman, K.H. Albertine, V.T. Winter, J.J. Coalson, J.D. Crapo, P.H. Grubb, P.W. Shaul, Inhaled NO improves early pulmonary function and modifies lung growth and elastin deposition in a baboon model of neonatal chronic lung disease, Am. J. Physiol. Lung Cell. Mol. Physiol. 288 (3) (2005) L450–L491.
[20] R.D. Bland, K.H. Albertine, D.P. Carlton, A.J. Macritchie, Inhaled nitric oxide effects on lung structure and function in chronically ventilated preterm lambs, Am. J. Respir. Crit. Care Med. 172 (7) (2005) 899–906.
[21] S.C. Land, C. Rae, iNOS initiates and sustains metabolic arrest in hypoxic lung adenocarcinoma cells: mechanism of cell survival in solid tumor core, Am. J. Physiol. Cell Physiol. 289 (4) (2005) C918–C933.
[22] J.A. Clements, M.E. Avery, Lung surfactant and neonatal respiratory distress syndrome, Am. J. Respir. Crit. Care Med. 157 (1998) S59–S66.
[23] T.E. Weaver, J.J. Conkright, Function of surfactant proteins B and C, Annu. Rev. Physiol. 63 (2001) 555–578.
[24] M. Kalina, R.J. Mason, J.M. Shannon, Surfactant protein C is expressed in alveolar type II cells but not in Clara cells of rat lung, Am. J. Respir. Cell Mol. Biol. 6 (1992) 594–600.
[25] J. Marcinkiewicz, A. Grabowska, B. Chain, Nitric oxide up-regulates the release of inflammatory mediators by mouse macrophages, Eur. J. Immunol. 25 (1995) 947–951.
[26] J.S. Colvin, A.C. White, S.J. Pratt, D.M. Ornitz, Lung hypoplasia and neonatal death in Fgf9-null mice identify this gene as an essential regulator of lung mesenchyme, Development 128 (2001) 2095–2106.
[27] M. Weaver, N.R. Dunn, B.M.L. Hogan, BMP4 and FGF10 play opposing roles during lung bud morphogenesis, Development 127 (2000) 2695–2704.
[28] M. Weaver, J.M. Yingling, N.R. Dunn, S. Bellusci, B.L. Hogan, BMP signaling regulates proximal-distal differentiation of endoderm in mouse lung development, Development 126 (1999) 4005–4015.
[29] D. Warburton, M. Schwarz, D. Tefft, G. Flores-Delgado, K.D. Anderson, W.V. Cardoso, The molecular basis of lung morphogenesis, Mech. Dev. 92 (2000) 55–81.
[30] J.S. Beckman, $^-$OONO: rebounding from nitric oxide, Cir. Res. 89 (2001) 295–297.
[31] J. Gao, B.X. Zeng, L.J. Zhou, S.Y. Yuan, Protective effects of early treatment with propofol on endotoxin-induced acute lung injury in rats, Br. J. Anaesth. 92 (2004) 277–279.
[32] J.F. Pittet, L.N. Lu, D.G. Morris, K. Modelska, W.J. Welch, H.V. Carey, J. Roux, M.A. Matthay, Reactive nitrogen species inhibit alveolar epithelial fluid transport after hemorrhagic shock in rats, J. Immunol. 166 (2001) 6301–6310.
[33] Y. Vodovotz, J.B. Kopp, H. Takeguchi, S. Shrivastav, D. Coffin, M.S. Lucia, J.B. Mitchell, R. Webber, J. Letterio, D. Wink, A.B. Roberts, Increased mortality, blunted production of nitric oxide and increased production of TNF-α in endotoxemic TGF-β1 transgenic mice, J. Leukoc. Biol. 63 (1998) 31–39.
[34] M.A. Perrella, C.M. Hsieh, W.S. Lee, S. Shieh, J.C. Tsai, C. Patterson, C.J. Lowenstein, N.C. Long, E. Haber, S. Shore, M.E. Lee, Arrest of endotoxin-induced hypotension by transforming growth factor β1, Proc. Natl. Acad. Sci. USA 93 (1996) 2054–2059.
[35] Y.H. Chen, M.D. Layne, S.W. Chung, K. Ejima, R.M. Baron, S.F. Yet, M.A. Perella, Elk-3 is a transcriptional repressor of nitric-oxide synthase 2, J. Biol. Chem. 278 (2003) 39572–39577.
[36] J. Massague, Y.G. Chen, Controlling TGF-β signaling, Genes Dev. 14 (2000) 627–644.
[37] E.M. Pera, A. Ikeda, E. Eivers, E.M. De Robertis, Integration of IGF, FGF, and anti-BMP signals via Smad1 phosphorylation in neural induction, Genes Dev. 17 (2003) 3023–3028.
[38] K.A. Waite, C. Eng, From developmental disorder to heritable cancer: it's all in the BMP/TGF-β family, Nat. Rev. Genet. 4 (2003) 763–773.
[39] X. Zeng, M. Gray, M.T. Stahlman, J.A. Whitsett, TGF-β1 perturbs vascular development and inhibits epithelial differentiation in fetal lung in vivo, Dev. Dyn. 221 (2001) 289–301.
[40] L. Zhou, C.R. Dey, S.E. Wert, J.A. Whitsett, Arrested lung morphogenesis in transgenic mice bearing an SP-C-TGF-β1 chimeric gene, Dev. Biol. 175 (1996) 227–238.
[41] R. Serra, R.W. Pelton, H.L. Moses, TGF-β1 inhibits branching morphogenesis and N-*myc* expression in lung bud organ cultures, Development 120 (1994) 2153–2161.
[42] B.C. Willis, J.M. Liebler, K. Luby-Phelps, A.G. Nicholson, E.D. Crandall, R.M. du Bois, Z. Borok, Induction of epithelial–mesenchymal transition in alveolar epithelial cells by transforming growth factor-beta1: potential role in idiopathic pulmonary fibrosis, Am. J. Pathol. 166 (5) (2005) 321–332.
[43] Y. Vodovotz, L. Chesler, H. Chong, S.J. Kim, J.T. Simpson, W. DeGraff, G.W. Cox, A.B. Roberts, D.A. Wink, M.H. Barcellos-Hoff, Regulation of transforming growth factor β1 by nitric oxide, Cancer Res. 59 (1999) 2142–2149.
[44] G.S. Warshamana, M. Corti, A.R. Brody, TNF-α, PDGF, and TGF-β1 expression by primary mouse bronchiolar–alveolar epithelial and mesenchymal cells: TNF-α induces TGF-β1, Exp. Mol. Pathol. 71 (2001) 13–33.